CONCEPTS FOR SMART PROTECTIVE HIGH-TEMPERATURE COATINGS

P. F. Tortorelli, M. P. Brady, I. G. Wright, and B. A. Pint
Oak Ridge National Laboratory

INTRODUCTION

Environmental resistance is a critical material barrier to the operation of fossil systems with the improved energy efficiencies and environmental performance described by the goals of the Vision 21 concept of the U.S. Department of Energy's Office of Fossil Energy. All fossil fuel-derived processes contain reactive species and high-temperature degradation arising from reactions of solids with gases and condensable products often limits performance or materials lifetimes such that efficiency, emission, and/or economic targets or requirements are not realized. Therefore, historically, the development of materials for fossil-fuel combustion and conversion systems has been closely linked to corrosion studies of alloys and ceramics in appropriate environments. This project is somewhat different from such studies in that it focuses on the feasibility of new routes to controlling the critical chemical and mechanical phenomena that collectively form the basis for environmental protection in relevant fossil environments by exploring compositional and microstructural manipulations and cooperative phenomena that have not necessarily been examined in any detail to date. This can hopefully lead to concepts for "smart" coatings or materials that have the ability to sense and respond appropriately to a particular set or series of environmental conditions in order to provide high-temperature corrosion protection.

The strategies being explored involve cooperative or in-place oxidation or sulfidation reactions of multiphase alloys.[1,2] The first material systems to be evaluated involve silicides as there is some evidence that such materials have enhanced resistance in oxidizing-sulfidizing and sulfidizing environments and in air/oxygen at very high temperatures.[3] In this regard, molybdenum silicides may prove to be of particular interest. Molybdenum is known to sulfidize fairly slowly[4] and there has been recent progress in developing Mo-Si-B systems with improved oxidation resistance at high and intermediate temperatures.[5–11] Consequently, Mo-Si-B alloys with different compositions and phase morphologies were oxidized in dry air at 1200°C under cyclic oxidation conditions. In addition, elevated-temperature oxidation-sulfidation exposures of Mo-Mo_5SiB_2-Mo_3Si alloys were also conducted. In this way, the specific effects of the multiphase nature (composition, morphology) of the Mo-Si-B system on protective product formation are being evaluated.

DISCUSSION OF CURRENT ACTIVITIES

Automated cyclic oxidation exposures were conducted on an α-Mo-Mo_5SiB_2-Mo_3Si alloy (from within the 3-phase field labeled "1" in Fig. 1) in dry, flowing O_2 at 1200°C using a cycle consisting of 60 min at temperature and 10 min out of the furnace. Duplicate specimens of the α-Mo-Mo_5SiB_2-Mo_3Si α-Mo-Mo_5SiB_2-Mo_3Si composition were attached to alumina rods with Pt-Rh wires and mass changes were typically measured after 1, 5, 40, 60, 80, and 100 cycles and then every 100 cycles using a Mettler model AG245 balance. The resulting gravimetric data are shown in Fig. 2, which also contains data from compositions based on the phase fields denoted as "2" and "3" in Fig. 1.[12,13] The specimens containing α-Mo showed a substantial mass loss for the first thermal cycle. Subsequently, only modest changes in specimen mass were measured. In fact, after the first cycle, the rates of mass change of the two α-Mo-Mo_5SiB_2-Mo_3Si specimens were equivalent to and less than those measured for the T1-Mo_5SiB_2-Mo_3Si coupons and not much different than that of the $MoSi_2$-containing alloy (Fig. 2). Such observations suggest a multistage mechanism in which the Mo is rapidly removed by formation of volatile MoO_3 and the resulting near-surface enrichment in silicon and boron facilitate the formation of a protective borosilicate or silica layer that grows laterally to seal the remaining Mo-rich areas of the alloy from the environment.[9] Results from short-term cyclic oxidation experiments were consistent with this interpretation—see, as an example, Fig. 3, which shows that the initial mass loss was dependent on the

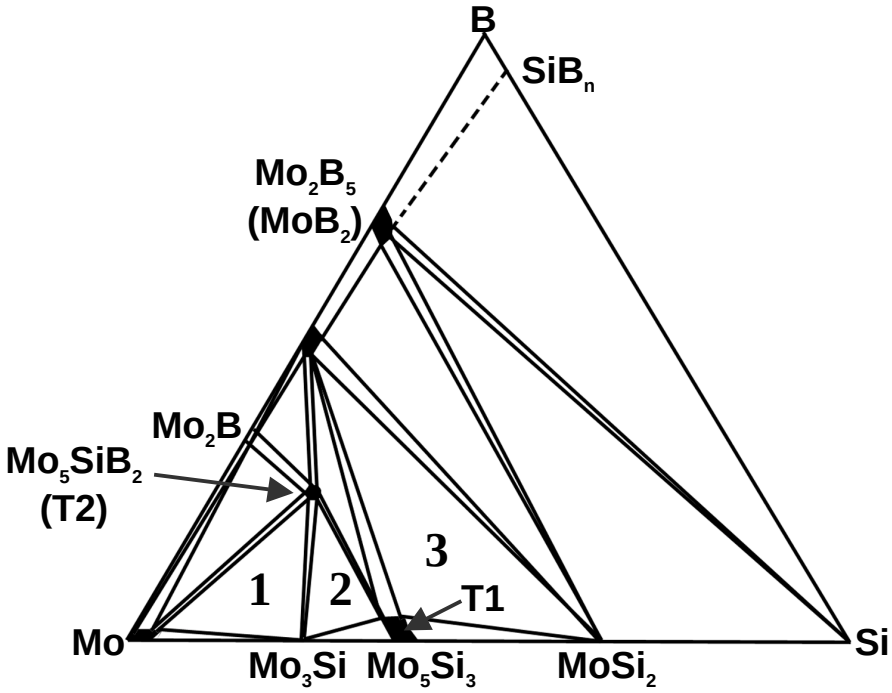

Fig. 1. A schematic Mo-Si-B phase diagram based on Nowotny et al., 1957.

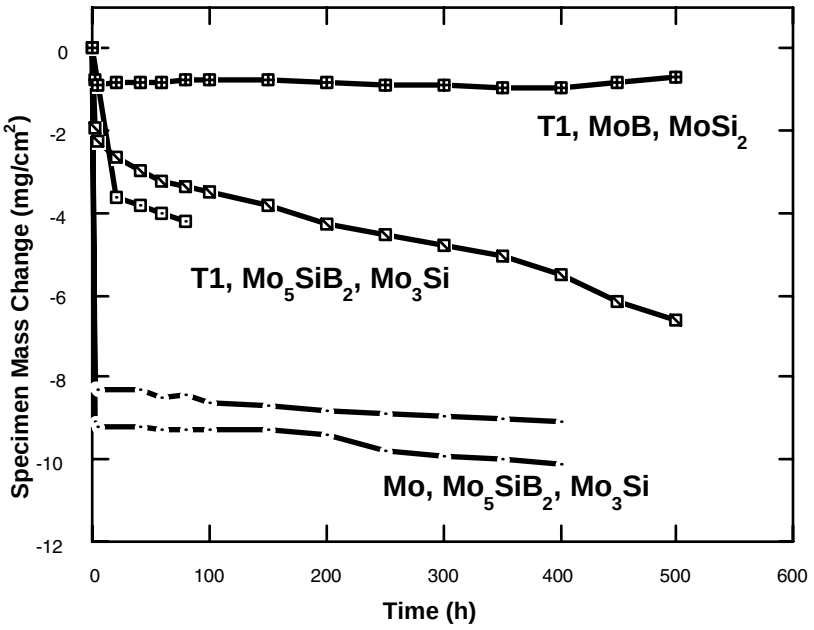

Fig. 2. Specimen mass change of Mo-Si-B alloys as a function of time at 1200°C for 1-h thermal cycles

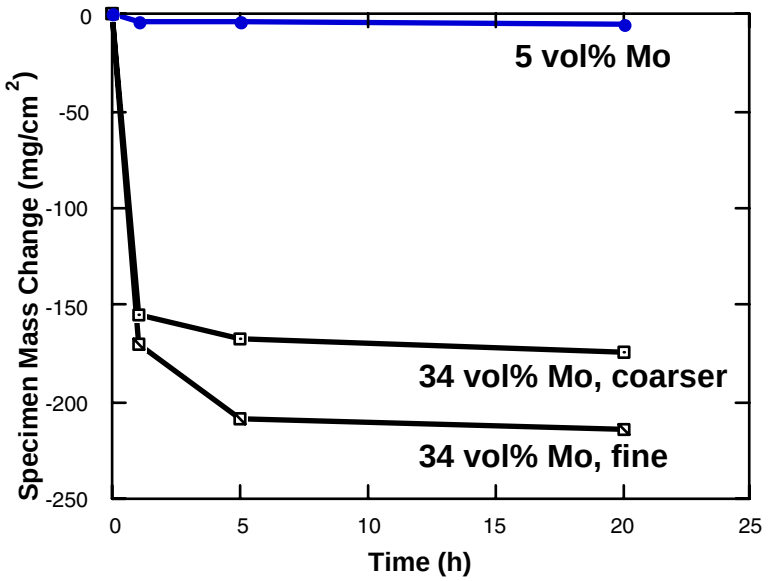

Fig. 3. Specimen mass change of Mo-Si-B alloys as a function of time at 1200°C for 1-h thermal cycles,[10] Fine and coarser refer to size of Mo phase in the 34vol% Mo alloys. See ref. 10 for examples of these microstructures.

starting Mo concentration and that the onset of protective behavior was indeed very rapid. This type of process suggests that the oxidation behavior of this multiphase system can possibly be controlled by finely dispersing not only the most active phase (α-Mo), but also the most Si-rich component, which can act as a source for silicon during oxidation,[11] based on the concepts of cooperative oxidation phenomena.[1,14] In this regard, Mo-Mo_5SiB_2-Mo_3Si alloys with a fine-scale microstructure have been shown to have significantly better oxidation resistance than similar compositions with a coarser phase dispersion.[10,11] However, the cyclic oxidation results shown in Fig. 3 do not show a significant difference between the behavior of two Mo-Mo_5SiB_2-Mo_3Si alloys that have the same Mo content (34%) but a fine and coarser microstructure, respectively. Accordingly, it is not presently clear whether manipulation of phase sizes to increase the oxidation resistance of these Mo-Si-B alloys will be effective (or practical, given that the need for improved fracture toughness appears to necessitate a coarser Mo phase [10]).

A preliminary evaluation of the sulfidation resistance of α-Mo-Mo_5SiB_2-Mo_3Si alloys was conducted by isothermally exposing specimens to an H_2-H_2S-H_2O-Ar gas mixture at 800°C for 100–150 h. At this temperature, the gas composition yielded a p_{S_2} of ~10^{-6} atm and a p_{O_2} of ~10^{-22} atm. This environment represents severe coal gasification conditions, but has been used previously to evaluate the corrosion of the most sulfidation-resistant alloys.[15,16] Furthermore, calculations based on equilibrium thermodynamics predict that Mo-Si alloys should form SiO_2 and MoS_2 under these conditions (Fig.4).

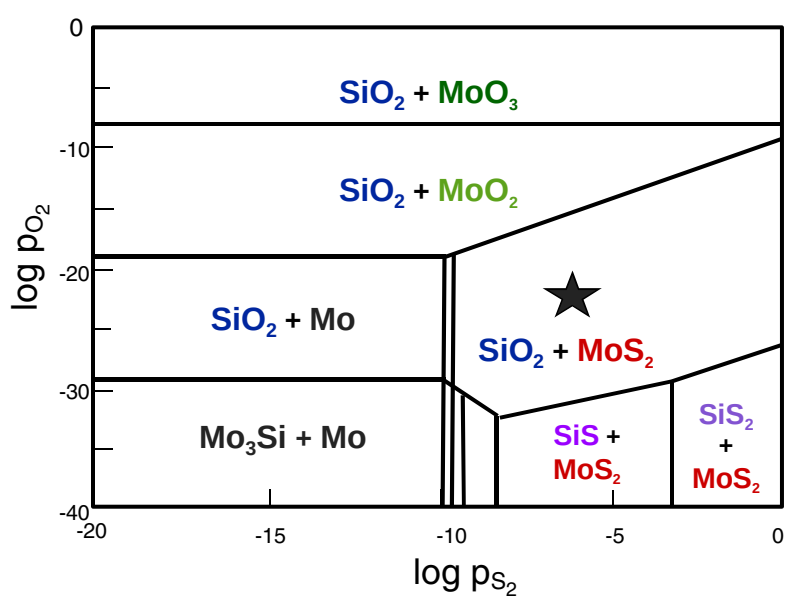

Fig. 4. Calculated product stability diagram for Mo-Si as a function of the partial pressures of oxygen and sulfur. The star represents partial pressures of H_2-H_2S-H_2O-Ar gas mixture used for oxidation-sulfidation exposures at 800°C.

The gravimetric results are shown in Fig. 5, which also includes typical data for a very sulfidation-resistant alloy, Fe_3Al,[15,17] another alumina-former (FeCrAl), and a model austenitic stainless steel (based on the nominal Cr and Ni concentrations of type 310). The different α-Mo-Mo_5SiB_2-Mo_3Si specimens (same Mo concentration, 34 vol%, but differing coarseness of the microstructure) showed similar gravimetric behavior representative of very good sulfidation resistance. Scanning electron microscopy of the as-exposed surfaces indicated only thin corrosion products (Fig. 6). (Little spallation was observed.) Because of the limited volume of these products, x-ray diffraction could not definitively determine their compositions, but it was apparent that some sulfides had formed. Interestingly, as shown in Fig. 6, the various phases appeared to react with the environment independently of each other. It therefore appears that, under the current oxidation-sulfidation exposure conditions, the α-Mo-Mo_5SiB_2-Mo_3Si alloys exhibit the "in-place" (or "independent") mode of multiphase oxidation.[1] Therefore, within the range of phase sizes investigated in this study, it is expected that the coarseness of the phase distribution should not have a major effect on corrosion behavior and this is what is observed in the gravimetric results (Fig. 5b)**.**

If confirmed by more comprehensive analytical work and exposures in aggressive varying environments, the knowledge gained about the different modes of reaction under oxidizing and oxidizing/sulfidation conditions (cooperative versus in-place, see above) will be used to help explore

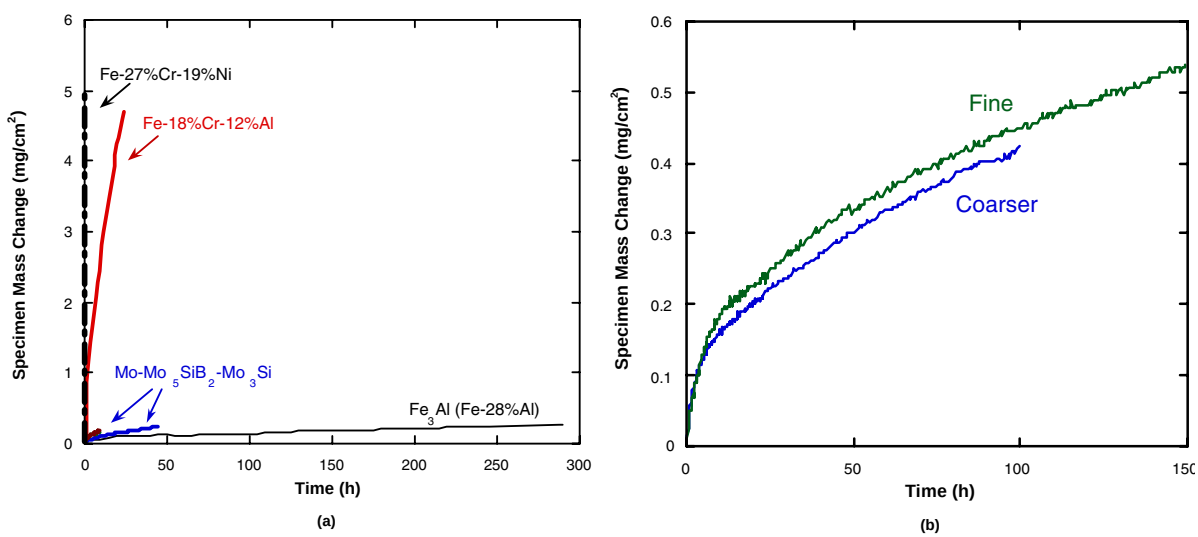

Fig. 5. Mass change versus time for exposures of Mo-Mo_5SiB_2-Mo_3Si, a stainless steel model alloy (Fe-27%Cr-19%Ni), and a FeCrAl (concentrations in at.%) to H_2-H_2S-H_2O-Ar at 800°C. (b) replots Mo-Mo_5SiB_2-Mo_3Si data of (a) with expanded ordinate scale. "Coarser" and "fine" refer to respective sizes of the phases in the Mo-Mo_5SiB_2-Mo_3Si alloys.

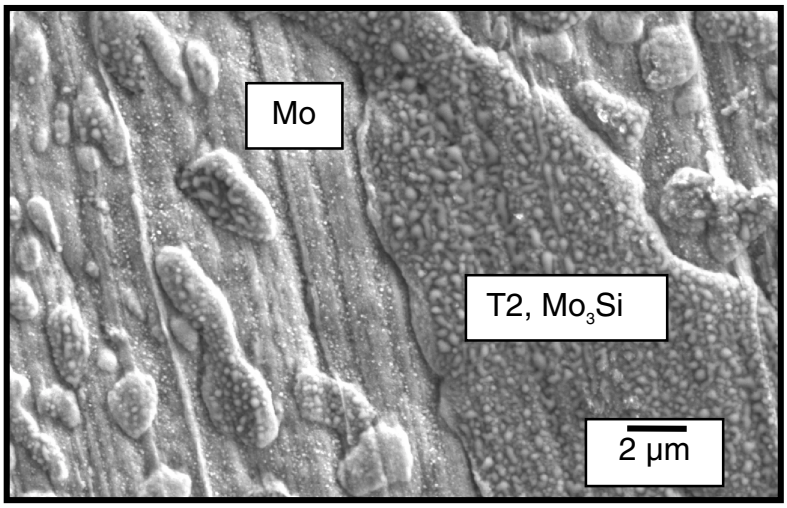

Fig. 6. Scanning electron micrograph of the surface of a specimen of Mo-Mo_5SiB_2-Mo_3Si after exposure to H_2-H_2S-H_2O-Ar at 800°C for 150 h.

phase and composition manipulations in the Mo-Si-B system in order to evaluate the possibilities of developing such alloys as smart protective coatings. Other multiphase alloys will also be examined for such coating applications based on opportunities to improve corrosion resistance through microstructure/geometric effects and alteration of subsurface depletion paths.[2]

SUMMARY

Smart protective coatings may provide one of the breakthrough areas to overcome materials barriers imposed by the requirements of advanced fossil energy systems. To this end, multiphase molybdenum silicides are being examined as the first attempt in evaluating smart coating concepts for high-temperature corrosion resistance in fossil environments. The present work confirmed that Mo-rich, B-containing silicides can have adequate oxidation resistance at high temperature. Also, preliminary results showed that these silicides have excellent high-temperature sulfidation resistance.

REFERENCES

1. F. Gesmundo and B. Gleeson, *Oxid. Met.* **44** (1995) 211–37.
2. M. P. Brady, B. Gleeson, and I. G. Wright, *JOM* **52** (2000) 16–21.
3. M. P. Brady, B. A. Pint, P. F. Tortorelli, I. G. Wright, and R. J. Hanrahan Jr., Chapter 6 in *Corrosion and Environmental Degradation of Materials*, M. Schütze (eds.), Wiley-VCH, Weinheim, Germany, 1999.
4. S. Mrowec, *Oxid. Met.* **44** (1995) 177–209.
5. M. K. Meyer and M. Akinc, *J. Am. Ceram. Soc.* **79** (1996) 938–944.

6. D. M. Berczik, “Oxidation Resistant Molybdenum Alloys,” U.S. Patent, 5,693,156, 1997.
7. M. K. Meyer, A. J. Thom, and M. Akinc, *Intermetallics* **7** (1999) 153–62.
8. K. Natesan and S. C. Deevi, *Intermetallics* **8** (2000) 1147–58.
9. M. G. Mendiratta, T. A. Parthasarathy, and D. M. Dimiduk, *Intermetallics* **10** (2002) 225–32.
10. J. H. Schneibel, P. F. Tortorelli, M. J. Kramer, A. J. Thom, R. O. Ritchie, and J. J. Kruzic, paper BB.2 in *Defect Properties and Related Phenomena in Intermetallic Alloys*, E. P. George, H. Inui, M. J. Mills, and G. Eggeler (eds.), The Materials Research Society, Pittsburgh, 2002.
11. V. Supatarawanich, D. R. Johnson, and C. T. Liu, *Mater. Sci. Eng. A* **344** (2003) 328–39.
12. P. F. Tortorelli, B. A. Pint, K. L. More, A. J. Thom, and M. Akinc, *ORNL Fossil Energy Program Annual Report for April 2000 to March 2001*, R. R. Judkins and P. T. Carlson (eds.), ORNL/TM-2001/89, July 2001, www.ornl.gov/fossil.
13. P. F. Tortorelli, M. P. Brady, I. G. Wright, and B. A. Pint, *ORNL Fossil Energy Program Annual Report for April 2001 to March 2002*, R. R. Judkins and P. T. Carlson (eds.), ORNL/TM-2002/122, July 2002, www.ornl.gov/fossil.
14. G. Wang, B. Gleeson, and D. L. Douglass, *Oxid. Met.* **35** (1991) 333–48.
15. J. H. DeVan and P. F. Tortorelli, *Mater. at High Temp.* **11** (1993) 30–35.
16. K. Natesan and P. F. Tortorelli, pp. 265–80 in *Nickel and Iron Aluminides: Processing, Properties and Applications*, S. C. Deevi, V. K. Sikka, P. J. Maziasz, and R. W. Cahn (eds.), ASM International, Materials Park, OH, 1997.
17. J. H. DeVan, pp. 107–15 in *Oxidation of Intermetallics*, T. Grobstein and J. Doychak (eds.), TMS, Warrendale, PA, 1989.